Offset Coupling, Feedback, and Spatial Multiplexing in 4 × 4 Incoherent-MIMO Multimode Fiber Links

Kumar Appaiah, *Student Member, IEEE*, Rodolfo Salas, Sriram Vishwanath, *Senior Member, IEEE*, and Seth R. Bank, *Senior Member, IEEE*

***Abstract*—We experimentally evaluate the performance of incoherent multiple-input multiple-output (MIMO) multimode fiber (MMF) links with different fiber media, link lengths, and modulation techniques. The performance of conventional 62.5 μm diameter silica as well as perfluorinated plastic, graded-index MMF sections of various lengths were evaluated using $1 \times 1, 2 \times 2, 3 \times 3$ and 4×4 MIMO setups over a range of lengths, with both open-loop equalization and feedback-based spatial multiplexing techniques. The data rate was evaluated over silica fiber sections with lengths ranging between 100 m–3 km using distributed feedback lasers and VCSELs at the transmitters. In addition, plastic optical fiber sections with lengths ranging from 1 m—100 m were evaluated with Fabry Perot lasers. Axial offsets were introduced while launching into, and detecting from the MMF to enhance modal diversity, and the impact of these offsets on the data rates was measured to obtain optimal launch and detection conditions. With optimized launch conditions and modulation parameters, the silica based systems realized data rates of 16 to 26 Gb/s, representing a bandwidth-length product improvement of $28\times$ over MMF standards such as 10 GBASE-SR. The plastic fiber system reached data rates of 24 to 43 Gb/s, with bandwidth-length product increases of up to $12\times$ of rated parameters. The use of off-axis launch and detection with flexible offsets on all four MIMO streams of the 4×4 system would enable further performance improvement.**

***Index Terms*—Optical fiber communication, MIMO.**

I. Introduction

THE growing demand for bandwidth has caused a significant rise in data rate requirements through various wireless and wired media. This has necessitated the rapid scaling of telecommunication networks, with newer optical components as well as better modulation and coding techniques. Optical fibers have proven to be effective in allowing high bandwidths to be sustained over short and long-haul links. In particular, single-mode fibers (SMFs) have been the primary drivers of long distance high-speed communication links which span up to several hundred kilometers, owing to their low loss and low dispersion properties [1]. However, for short and medium range links ranging from hundreds to few thousands of meters, deploying SMF solutions proves to be expensive because sub-micron alignment tolerances imposed by small-core diameter SMFs causes device costs to become prohibitive. Conventional multimode fibers (MMFs), on the other hand, possess a much larger core diameter (typically 50 μm or 62.5 μm), thus obviating the tight alignment tolerances and have the potential to enable low cost links. However, their large core diameter causes the signal to propagate over several fiber modes with different group velocities, thus significantly limiting data rates. While techniques such as dispersion compensation mitigate the dispersion effects to some degree, a significant improvement in data rates over MMFs requires improved signaling techniques, such as multiple-input multiple-output (MIMO) communication. Moreover, the use of MIMO along with advanced signal processing allows flexibility in the choice of various modulation and coding parameters which can be dynamically tuned for optimal resource utilization.

The application of MIMO techniques to MMFs was first investigated in [2], where the utility of MIMO was demonstrated, albeit at modest data rates. Subsequently, coherent as well as incoherent approaches to detection have been shown to be useful for MIMO-MMF links. Coherent MIMO implementations involve heterodyne detection, requiring the recovery of the original laser signal in phase. This approach has been demonstrated to be effective in conventional (large-core) multimode fibers [3], [4], as well as modern fibers, such as few-mode and multi-core fibers [5]–[11]. Coherent MIMO implementations in single mode fibers have been realized using polarization diversity [12], [13] and orthogonal band multiplexing [14], [15]. A simpler incoherent communications approach, based solely on intensity modulation and direct detection, obviates the need for laser signal recovery [16]–[19], and this is the approach used for the experiments discussed in this paper. These methods have allowed the benefits of MIMO signaling to be harnessed with much lower deployment complexity, at the cost of diminished multiplexing benefits due to incoherent square-law detection. Launching into the MMF with a radial offset to the fiber axis, with the aim of improving the bandwidth-length product while using intensity modulation and direct detection has been considered for silica fibers [20]–[22]. It has also been demonstrated that data throughput through plastic MMF can be significantly improved with the use of signal processing [23]–[25], and the use of MIMO techniques to provide further improvements has also been proposed [26]. However, a comprehensive evaluation of channel quality and the impact of changing fiber length, launch offset and the use of advanced modulation and signal processing techniques over different MMF media is yet absent.

Characterization of the impact of link parameters such as wavelength, fiber material, modulation and coding and axial

Manuscript received March 14, 2013; revised June 02, 2013; accepted July 23, 2013. Date of publication July 25, 2013; date of current version August 14, 2013. This work was supported by the National Science Foundation under an EAGER grant (EECS-1230034). This work was presented in part at the Optical Fiber Communications (OFC) Conference, March 2013, Anaheim, CA, USA.

The authors are with the Department of Electrical and Computer Engineering, The University of Texas at Austin Austin, TX 78712 USA (e-mail: kumar.a@utexas.edu).

Color versions of one or more of the figures in this paper are available online at http://ieeexplore.ieee.org.

Digital Object Identifier 10.1109/JLT.2013.2274795

offsets on fiber data rates is essential in understanding the capabilities and limitations of incoherent MIMO-MMF links. In this paper, we have described a detailed experimental evaluation of the impact of varying these parameters and how this data leads to conclusions on developing more effective multiplexing and dispersion compensation solutions for incoherent MIMO-MMF links. Data rates were measured on 2×2, 3×3 and 4×4 MIMO-MMF links that used silica graded-index MMF (GI-MMF) sections with lengths ranging from 100 m to 3 km, and 1×1 and 2×2 links with plastic GI-MMF sections of length 1 m to 100 m. To facilitate convenient evaluation using the evaluation setup, all fiber sections evaluated had a diameter of 62.5 μm. Controlling the axial offset during launching signals into, and detection of signals from the output of the fiber allowed the launched modal distribution to be altered. This approach closely parallels the technique of antenna placement in wireless MIMO, where appropriate placement of antennas is essential to ensure that multiplexing gains can be achieved [27]. In addition to fiber offsets, mode scramblers were also employed to further increase modal diversity. The silica links were evaluated with a distributed feedback (DFB) laser and vertical-cavity surface-emitting lasers (VCSELs), while the plastic fiber links were realized using a Fabry-Perot laser (FPL). The MIMO techniques described in this paper resulted in a bandwidth-length improvements ranging from $10\times$ to $28\times$ over the rated fiber bandwidth-length product (that corresponds to the data rates obtainable using on-off keying on a 1×1 system).

The rest of this paper is organized as follows: In Section II, we describe the metrics evaluated to characterize the properties of the MMF link. Section III describes the components of the optical system as well as the signal processing and modulation/coding parameters used in the system. Section IV describes the actual experimental results. Section V provides a discussion of the experimental results and puts them in the context of developing improved datacom solutions for MMF links. Finally, Section VI summarizes results and discusses some future directions.

II. Metrics for Evaluating MIMO-MMF Systems

In this section, we describe the channel models and metrics used to evaluate the In optical MIMO literature, the term "spatial multiplexing" is often used in the context of MMF links to refer to directly multiplexing using the modes of the fiber. However, in this paper, we use the definition of spatial multiplexing from the wireless MIMO context, as defined in [27], where the physical channel is mathematically parallelized into several virtual parallel channels to facilitate transmission of multiple streams in conjunction with signal processing. This definition is appropriate for characterizing the multiplexing capabilities of the fiber channel in the case where information about the fiber channel state is made available to the transmitter.

In order to evaluate and compare various system parameters, we first present the abstraction used as part of the signal processing structure during the encoding and decoding process. These parameters provide a means to directly view how the channel states of the fiber and the various transformations that it effects translate to changes in data rate and multiplexing capabilities of the system. A key difference in the approach described here is that we do not transmit and receive directly on the physical MIMO channels, but we transform them to virtual parallel channels and transmit and receive information on these processed channels. Thus, the resources of the physical channels are efficiently utilized to facilitate efficient transmission and reception signals over these processed virtual channels.

To simplify the implementation and description, we utilize a subcarrier based approach, in this case, orthogonal frequency division multiplexing (OFDM), since it has been demonstrated that OFDM is effective in combating dispersion in MMF links [28], [29]. This allows each subcarrier to possess a single-tap (flat-fading) channel parameter, thus making per-subcarrier equalization just a process of dividing by the estimated channel value, for zero-forcing equalization. In our implementation, we used minimum mean-square equalization to correct for channel impairments.

The use of incoherent detection constrains the signals transmitted and detected at the received to be real and non-negative. To arrive at a more conventional approach to modulation, we perform transform the channel using an approach described in [28]. We briefly describe this transformation here. The non-negative signal at the receiver is viewed as a real signal possessing a bias. Thus, we recalibrate the signal axis to allow positive and negative values for modulation. Fig. 2 shows an example of this situation, the intensity values between 0 and $I_{\max}$ offset by $I_{\max}/2$, to obtain a signal that varies between $\pm I_{\max}/2$.

Further, since we use baseband signaling, we require the OFDM signal to be real. To ensure that this is the case, we enforce the following condition on the complex modulated N_{FFT} subcarriers $X[0], X[1], \ldots, X[N_{\mathrm{FFT}} - 1]$ of each OFDM symbol:

$$X[N_{\mathrm{FFT}} - k] = X[k]^*, \quad k = 1, 2, \ldots, N_{\mathrm{FFT}}/2, \qquad (1)$$

where a^* denotes the complex conjugate of a. The constraint in (1) halves the spectral efficiency by a factor of two. In addition, the transformation described in Fig. 2 prevents the use of the dc subcarrier ($X[0]$) for data transmission. Despite these limitations, the use of OFDM on intensity modulation/direct detection based optical links is known to be effective in increasing data rates over optical fiber links [28], [30]–[33].

With this system model, we can view each subcarrier as a conventional flat-fading MIMO channel. In the following discussion, we suppress the subcarrier number, and use notation consistent with [27]. For an M-transmitter N-detector MIMO system, let $\mathbf{H}$ be the $N \times M$ MIMO channel matrix for a subcarrier. To characterize the system from a spatial multiplexing perspective, we use the singular-value decomposition (SVD) of the channel matrix. The SVD of the channel matrix $\mathbf{H}$ can be represented as:

$$\mathbf{H} = \mathbf{U}\mathbf{\Sigma}\mathbf{V}^* \qquad (2)$$

where $\mathbf{U}$ and $\mathbf{V}$ are unitary matrices, and $\mathbf{\Sigma} = \mathrm{diag}\{\sigma_1, \sigma_2, \ldots \sigma_{\min(M,N)}\}$ is a $N \times M$ diagonal matrix containing non-negative elements on its diagonals, called

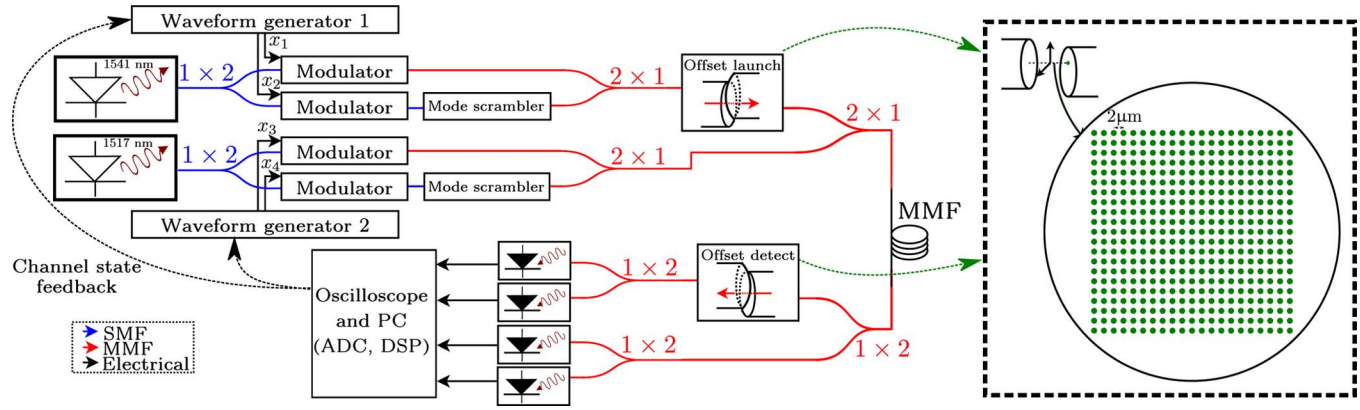

Fig. 1. Schematic of the 4 × 4 MIMO experimental setup. The offset launch and detection components were realized using nanoprecision fiber alignment stages, while the MMF couplers were all 2 × 1 couplers. The inset shows the offset positions for the launch and detect stages, which were placed in a square grid with offset intervals of 2 μm. Fibers and couplers colored blue represent SMF, while red represents MMF.

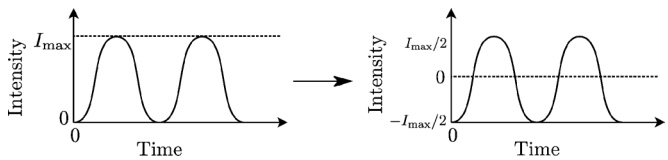

Fig. 2. A transformation to allow non-negative values with intensity modulation. Such a transformation permits all transmitted and received signals to be real signals, rather than purely non-negative signals.

singular-values. With this new formulation, the achievable rate over this subcarrier can be expressed as:

$$R = \sum_{i=1}^{\min(M,N)} \log_2\left(1 + \frac{P_i}{W}\sigma_i^2\right) \text{ b/s/Hz}. \qquad (3)$$

where P_i is the effective received power on each stream, and W is the noise variance. This formulation is similar to the wireless MIMO case with full CSI, as described in [27] and [34]. P_i/W can be understood as the effective signal-to-noise ratio (SNR) for each stream, if the each element h_{ij} of $\mathbf{H}$ is normalized to satisfy $\mathbb{E}[|h_{ij}|^2] = 1, i = 1, 2, \ldots N, j = 1, 2, \ldots M$; where $\mathbb{E}[\cdot]$ is the expectation operator.

Thus, we can view the MIMO channel from a multiplexing perspective as several parallel virtual channels whose SNRs are determined by the singular-values. While this formulation makes the assumption of a linear system, this assumption has been found to hold for intensity modulation systems under mild conditions [2], [35], [36]. Thus, with an experimental setup of a MIMO-MMF system, the above formulation provides us with metrics that allow for a detailed study on how changing various system parameters, such as launching and detector stage offsets, mode scramblers, modulation choices etc. affect the achievable data rate. In the following sections, we describe the design of such a link and describe the techniques we use to optimize the link to achieve the for maximum data rate using this formulation.

III. System Description

In this section, we describe the design and implementation of a 4 × 4 MIMO-MMF system, describing the various components as well as the modulation, coding and receiver aspects.

A. Optical System

Since the system is operated with various different fiber media and configurations, each of these is described separately.

1) Silica MMF With DFB Lasers: The optical system schematic for a 4 × 4 link with silica fibers is shown in Fig. 1. The transmitter consists of two (non-identical) C-band fiber coupled distributed feedback (DFB) lasers. The specific lasers used were a 1541 nm JDSU telecom laser and an NEL 1517 nm telecom laser, each having an optical power output of 13 dBm (20 mW). Two lasers were employed because the power requirements for links above 1 km could not be met by splitting a single laser for a 4 × 4 system. Moreover, the use of lasers carriers spaced apart more than the bandwidth of the signal minimizes the coherent interference among modes [17]. The optical signal from each of these lasers was split into two parts using SMF splitters. The four resulting signals were modulated using external intensity modulators, whose rf input signals were produced using two Tektronix 7102 arbitrary waveform generators from four quadrature amplitude modulated (QAM) data streams. The modulators used in this setup were four JDSU Mach-Zehnder modulators rated for 10 Gb/s operation. The two pairs of signals were then coupled together, with one of them connected to the coupler using a conventional patch cord and the other connected through a mode scrambler to induce a different mode profile [37]. The mode scramblers consist of tightly wound multimode fiber (consisting of about 100 turns, each of radii less than 1 cm) that are designed to facilitate heavy intermodal coupling in the transmitted signal, resulting in the randomization of modal content. Inducing a different mode pattern among each of the signals through a modal filtering or scrambling process serves to differentiate the spatial mode content of each data stream [2]. Distributing the signal across different modes, maintaining mechanical stability of the fiber, and the ability to perform digital signal processing at the receiver make the system robust against coherent modal interference [17]. After combining the two pairs of signals originating from each laser, these were further combined by means of an MMF coupler; one of them was butt-coupled, while the other was launched with a specific offset using a 3-axis nanoprecision fiber alignment stage. The optical signal thus

obtained was then transmitted and received over a conventional 62.5 μm diameter graded-index multimode fiber (OM1), whose rated bandwidth-length product was 2 Gb/s-km at 1550 nm and 1 Gb/s-km at 850 nm. This class of fibers is commonly deployed in 10 GBASE-SR systems [38].

On the receiver side, the signals were split using a MMF coupler, and one of these arms was butt-coupled into another MMF coupler directly, and the other was connected to an MMF coupler via a nanoprecision fiber alignment stage that acted as a modal filtering system. The resulting four signals were directly detected by four 10 Gb/s fiber coupled InGaAs photodetectors. Each photodetector's electrical output was connected to a Tektronix DPO70604 oscilloscope, which acted as an analog to digital converter (ADC). The detected signals were processed offline with signal processing algorithms. To obtain an accurate bit-error rate (BER) statistic, the transmission characteristics were evaluated over several thousand OFDM symbols, and the accumulated errors from these iterations were averaged to obtain a BER estimate. Feedback of channel state information, obtained using training symbols (pilots) at the receiver, was returned to the transmitter for the experiments where channel state was used at the transmitter. The temporal variation of the channel was measured, and it was found that channel estimates did not vary appreciably over about 2 milliseconds. Quantizing the channel state feedback to use 10 Mb every second allowed the feedback algorithms to function at a sufficient speed to sustain the data rates evaluated in our experiments. This corresponded to an overhead of 0.1% of the data rate. The transmission of each stream by the waveform generator was at 10 gigasamples/s, while the receiver sampling of the electrical output from the photodetectors at the oscilloscope was at 20 gigasamples/s. The fiber offset locations at the launch and detect fiber alignment stages were spread over a 40 μm $\times$ 40 μm grid, as shown in the inset of Fig. 1. The data rate was evaluated by launching and detecting at 2 μm offsets at the transmit and receive alignment stages, so as to obtain the best data rate.

The DFB laser based system's performance metrics and data rate capabilities were investigated over a wide array of fiber lengths; specifically 10 m, 100 m, 500 m, 1 km and 3 km. The various MIMO configurations ranging from 1 $\times$ 1 to 4 $\times$ 4 were obtained with slight modifications to the system in Fig. 1 as follows:

- 1 $\times$ 1: The couplers were removed from transmit and receive ends, and only the first laser was used at 10 dBm output power.
- 2 $\times$ 2: Streams x_1 and x_3 were used, along with the first and third photodetector directly connected (without couplers). The two lasers each operated at 10 dBm output power and the modulators and photodetectors were connected directly without couplers.
- 3 $\times$ 3: Streams x_1, x_2 and x_3 were used, along with the first three detectors. The first laser operated at 13 dBm, and was split by a 2 $\times$ 1 coupler, while the second laser operated at 10 dBm and was directly connected to the modulator corresponding to stream x_3.
- 4 $\times$ 4: The full system as, shown in Fig. 1, was active, with each laser output set to 13 dBm.

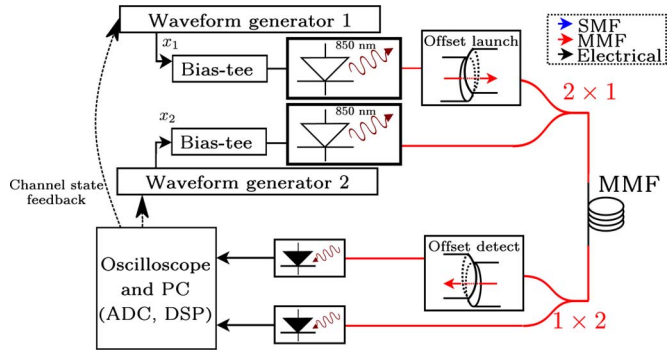

Fig. 3. The transmitter and receiver arrangement for the VCSEL case.

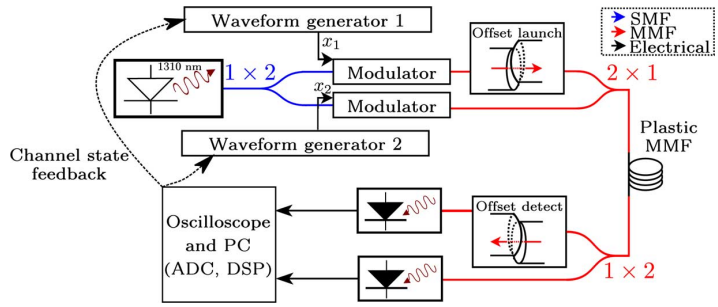

Fig. 4. The transmitter and receiver arrangement for the evaluation of plastic fibers.

The power levels of the lasers were adjusted to launch the same amount of power fiber per stream, for a fair comparison. The combined coupler and scrambler insertion losses were less than 1 dB, and thus, did not appreciably alter our data rate measurements.

2) Silica MMF With VCSELs: For the VCSEL case, the system design was fairly similar to the DFB based system, except that a 2 $\times$ 2 system was employed. The optical transmit subsystem consisted of two Finisar 850 nm VCSELs, each of which was biased and directly modulated by means of a 100 Hz–12 GHz bias-tee. The VCSELs were capable of emitting at -3 dBm (0.5 mW). The system is shown in Fig. 3. For the 1 $\times$ 1 case, the couplers were removed from both the transmitter and receiver, and only one VCSEL and detector were used.

The VCSEL based system's performance metrics and data rate capabilities were investigated over only 10 m, 100 m, 500 m and 1 km MMF fiber sections. Longer lengths were not considered since the optical power of the VCSELs was insufficient to support a sufficiently large SNR with longer fiber sections to ensure reliable communication at high speeds.

3) Plastic MMF With Fabry-Perot Laser: In addition to evaluating the system parameters for conventional silica MMF, a similar experiment was performed for a 2 $\times$ 2 optical link with a plastic MMF. The schematic for this setup is shown in Fig. 4. Like in the VCSEL system, for the 1 $\times$ 1 case, the couplers were removed from both the transmitter and receiver, and only one VCSEL and detector were used.

For these evaluations, perfluorinated graded-index plastic optical fiber with 62.5 μm diameter was used. This choice was made to allow for consistency in the use of components across

the silica and plastic fiber setups, and to facilitate comparison with the 62.5 μm diameter silica GI-MMF used in the other experiments. The rated bandwidth-length product of this fiber was 200 Mb/s-km, and the experiment was conducted on sections of length 1 m, 10 m and 100 m. The laser used was a single-mode fiber coupled 10 dBm (10 mW) Fabry Perot laser whose wavelength was 1310 nm, and the modulator was a JDSU lithium niobate external modulator designed for use in the O-band (1260–1360 nm).

4) Mode Scramblers and Fiber Offsets: The primary benefit of MIMO for data transmission through MMFs is obtained by separating multiple streams through different modes or mode groups of the fiber. To facilitate this, we took two approaches: the use of mode-scramblers and axial offset-launch and detection.

Passing an optical signal through a mode-scrambler causes the signal to gain a randomized modal footprint [37], [39]. The aim of using multiple mode scramblers, each producing a random mode footprint, was to allow signals to possess spatial diversity by virtue of traveling through different modes. The significant advantage of using mode scramblers is that they are easy to interface with an existing fiber-coupled setup. However, they are limited in the variation of modal footprint they provide, since they offer no means to alter or control the modal transformation they effect.

The use of fiber alignment stages at the transmitter and receiver provides a convenient means to evaluate the complete spatial characteristics of the fiber channel. By traversing all lateral offsets during signal launch and detection into the fiber, they can provide fine-grained access to the mode-groups of the fiber, along with simultaneous control at the transmit and receive stages to maximize the data rate. However, they also significantly complicate the deployment of the optical link. Our motivation in the use of the optical stage was to determine how offset coupling enhances the fiber data rates, and to gain intuition on geometries for the design of device structures (such as arrays of lasers and detectors) that would possess the combined benefits of enhanced data rates as well as deployment ease. It must be noted that the use of fiber alignment stages by themselves does not allow for access to individual modes or mode groups of the fiber. Modulating individual modes would require sophisticated techniques, such as spatial light modulation or accurate spatial filters, and would make the system highly sensitive to fiber variations and require tight alignment tolerances. Since the focus of these experiments is to utilize a diversity of modes rather than specific modes, we utilize offset launch and detection and do not focus on matching accurately to individual fiber modes or mode groups.

Launching and detection with offsets larger than a few microns results in a reduction of power coupling at the offset stages. However, offsets also result in an improvement in the diversity of modes excited during launch, resulting in improved multiplexing performance. The experiments described in the following sections measure this tradeoff, since the channel estimates and measured data rates recorded are based on the signal detected at the receiver. Since the SNRs are based on the measured power in each stream for the same transmit power, they accurately account for the losses incurred during offset coupling. This approach was used to permit characterization of the performance improvements over conventional (large-core) MMF systems operated at rated parameters.

TABLE I
OFDM SYSTEM PARAMETERS

Sampling rate	10 GS/s
FFT Size	128
Cyclic Prefix	5
Occupied subcarriers	58 (including 4 pilot subcarriers)
Constellation	QAM-2, 4, 8, 16, 64
Reed-Solomon code	(255, 239), (255, 231) and (255, 223) codes

B. Modulation and Coding

In this section, we discuss the modulation and coding utilized in the system implementation, as well as the MIMO techniques used for system evaluation and data rate measurements.

To simplify the design of the transmit and receive communication subsystems, orthogonal frequency division multiplexing (OFDM) and quadrature amplitude modulation (QAM) were employed to obtain a high spectral efficiency, and a Reed-Solomon code of appropriate rate to limit the BER. The constellations were chosen by waterfilling across subcarriers, and the highest rate Reed-Solomon code that achieved a BER of 10^{-9} was then used. The use of OFDM in optical communication has been shown to be a useful technique considered in the past both with coherent detection [40] and incoherent detection [41]. Since direct detection imposes the constraint that signals should be non-negative, the dc subcarrier was not used for data transmission, and the signal was offset to modulate the non-negative intensity of the laser. To facilitate channel estimation, some subcarriers were designated as "pilot" subcarriers, which carried symbols known to the receiver. One pilot was introduced for every 16 data subcarriers, and the channel estimates for the other subcarriers were obtained by interpolation. This choice was made based on the dispersion rating of fibers up to 3 km, which was the longest silica fiber section length evaluated in these experiments. This pilot allocation was experimentally determined to be sufficient to estimate the frequency selective nature of the channel. The receiver utilized these subcarriers to obtain a minimum mean-square error (MMSE) estimate of the channel parameters for these subcarriers and interpolated to determine the channel coefficients for the remaining subcarriers. The receiver data was collected and stored, and signal processing algorithms were executed offline on these to recover the transmitted data. To evaluate the data rate that can be obtained for a certain configuration of the system, the best combination of forward error correction (Reed-Solomon codes of appropriate rates) and modulation to yield the highest data rates was utilized. Thus, the measured data rates reported from the experiments are net data rates which account for channel training and forward error correction overheads so as to obtain a BER of 10^{-9} or lower. The exact parameters used for the OFDM system are listed in Table I.

To evaluate the system from a MIMO perspective, we utilize the spatial multiplexing technique described in Section II. First, channel measurements were obtained at the receiver by utilizing the pilot symbols. Using this channel coefficient data,

the achievable data rate through each subcarrier was calculated and added up to obtain a net achievable data rate estimate. In addition, by studying the singular values of the system, an inference can be drawn on how effective various virtual streams are in their ability to transmit data. These metrics are evaluated with various configurations of the optical system described above, including mode scramblers as well as various offset launching and detecting, as shown in the inset of Fig. 1. Once we obtain a position where the parameters are optimized, we evaluate the data rate obtained by optimizing the modulation and error control coding parameters.

For the data rate experiments, the techniques evaluated included:

- The vertical Bell Labs layered space-time (V-BLAST) code, which is an open-loop multiplexing technique that does not require feedback of channel coefficients. The decoding technique in this case is called successive interference cancellation. A detailed description of this technique can be found in [42].
- The feedback based spatial multiplexing technique, which uses feedback of channel coefficients to parallelize the channel, as described in Section II. The key advantage of this technique over V-BLAST is that it results in focused allocation of resources along the virtual parallel channels which offer the highest SNR, although the complexity of transmitting channel coefficients accurately to the transmitter makes it more difficult to realize massive gains in practice. These techniques are covered in detail in [27].

Channel state information was found at the receiver by sending an OFDM symbol with pilots on all subcarriers. The channel estimates thus obtained at the transmitter were immediately used for modulating further data for the feedback based spatial multiplexing case. The delay in transmission of the feedback information was within a few hundred milliseconds, to minimize the impact temporal channel variations. The temporal stability of the MMF channel is well known [3], [43], thus ensuring that the delay in feedback transmission is well within the coherence time of the system. This ensured that feedback transmission was useful for effective preprocessing at the transmitter.

To transmit feedback information to the transmitter, a simple approach of quantizing the channel estimates and relaying them to the transmitter was used. For obtaining an accurate estimate of channel coefficients, an OFDM symbol with pilots on all subcarriers was sent, so that the receiver could infer information about the channel state of every subchannel. This was followed by the actual data transmission, with modulation parameters optimized based on the channel state information. The accuracy of quantized feedback has a significant impact on the performance of a feedback based MIMO link [44], although a simple quantization approach is sufficient for us to demonstrate the value added by feedback in MMF-MIMO links, while retaining ease of practical implementation. Another significant fact utilized in this experiment was that the link coherence time, during which the channel coefficients are assumed to not change appreciably, is sufficiently large for the feedback of channel coefficients to be useful [3], [43]. Since the transmission requirements of the feedback channel generally amounts to a small fraction of the data rate, the burden of additional overheads incurred due to the transmission of feedback information is very small (0.1% in our case). The simplistic quantization approach described here results in noisy channel estimates, so an additional equalization step was performed at the receiver to compensate for this before the data was decoded. Exploration of feedback transmission methods that are specifically suited for optical links is a topic currently under investigation.

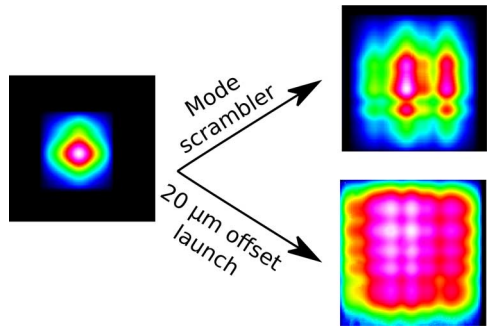

Fig. 5. The impact of a mode scrambler compared with a fiber offset launch after propagating through a 1 m MMF patch cord. While the mode scrambler causes an expansion of the beam and signal spread into neighboring modes, the alignment stage allows control for excitation of higher order modes.

For each of the transmission scenarios described above, the data rate was evaluated for the best combination of QAM modulation and Reed-Solomon code to obtain the maximum possible data rate, for various MIMO configurations and fiber lengths.

IV. Experimental Results

This section discusses in detail the results of each experiment conducted within the scope of this paper. Initially, we describe the common procedure for all experiments, and then discuss the specific performance results for various hardware and fiber media.

In our experiments, we also compare the performance results obtained by employing only mode scramblers and no fiber alignment stages, in order to characterize the mode diversity benefits provided by these solutions. In general, it was observed that while mode scramblers and the inherent asymmetry in mode couplers introduces some mode changes, they fall short of the diversity benefits obtained by the flexible control of offsets with fiber alignment stages. The example shown in Fig. 5 shows the output of a laser beam after propagation through an MMF for two cases: one after passing through a mode scrambler, and the other after launching into a patch cord with an axial offset of 12 μm before connecting to the MMF coupler. While a mode scrambler allows access to the modal diversity of an MMF without advanced components, the use of offset launch provides finer control, and is likely to result in better data rates.

The fiber system was set up for each experiment as indicated in Figs. 1, 3 and 4. The fiber alignment stages were computer controlled, and measurements of channel parameters and data signals were obtained by programmatically moving the fiber alignment stages over a 40 μm $\times$ 40 μm grid, with an increment of 2 μm between grid locations, as shown in the inset of

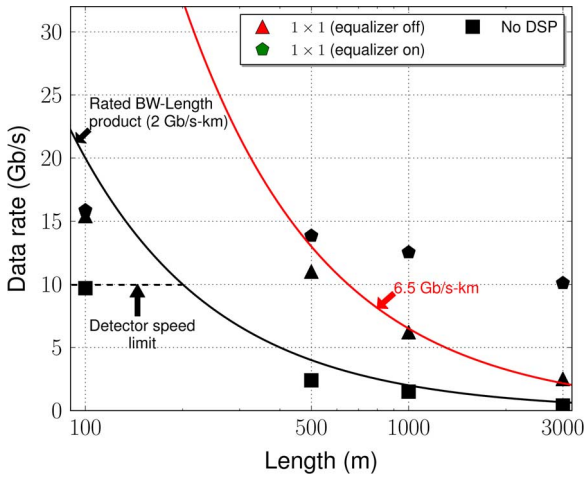

Fig. 6. Data rate versus length for a 1 × 1 system with and without signal processing.

Fig. 1. Before we delve into a detailed discussion of the experimental results, we discuss some of the limitations in measurements caused by speed restrictions imposed by the rf components of the system.

Fig. 6 compares the performance of a 1 × 1 MMF link of various lengths, with "No DSP" referring to conventional on-off keying without dispersion compensation (as in the case of 10GBASE-SR systems [38]), "equalizer off" referring to the case where OFDM with QAM modulation was used without performing performing an equalization of the channel effects on the subcarriers at the receiver, and "equalizer on" referring to a complete minimum mean-squared error equalization on a per-subcarrier basis. There are some important observations that can be made from these observations:

- The achieved data rate does not exceed the rated bandwidth-length product of the fiber for short lengths (around 200 m or less). This can be attributed to the fact that at short lengths, the data rate limitation is primarily due to restrictions in the maximum bandwidth of the signals generated by the waveform generator and the speeds of the modulators and detectors (a combined limitation of 7 GHz). For longer lengths of fiber, dispersion impacts the link more significantly, and becomes the dominant effect contributing to signal impairment for lengths of over 200 m.
- The benefits of using signal processing for dispersion compensation rise with increasing distance. From the figure, it is clear that the pulse shaping and spectrally efficient signaling with OFDM raises the bandwidth-length product to about 6.5 Gb/s-km. However, with dispersion compensation, the performance benefits over the "no equalization" case rise with distance, indicating that the benefits of using signal processing increase as fiber dispersion affects the system more significantly.

Therefore, in all our experimental results, we make a distinction between these two data transmission regimes: one where the system is limited by the equipment speed, and the other, where it is limited by fiber dispersion.

We now discuss data rates measured on these systems and their implications on the design of MIMO-MMF links.

A. 4 × 4 Link Over Silica MMF With DFB Lasers

The link shown in Fig. 1 was evaluated with and without offset launch, and the performance of V-BLAST as well as feedback based spatial multiplexing was considered. Each of the DFB lasers used was fiber coupled to a single-mode fiber, with a core diameter of 8 μm and a numerical aperture of 0.14, thus resulting in a beam which was very small in comparison to the core diameter of the MMF, which is 62.5 μm. The small beam size allowed fiber alignment during the launch stage to be effective and offered a significant control over the mode profile that could be obtained.

1) Impact of Offset Coupling on Multiplexing: As part of the experiment described here, we conducted a detailed measurement and analysis of how offset launch and detection improves data rate performance. Initially, the launch conditions were configured such that the fiber alignment stage at the transmitter, shown in Fig. 1, was fixed to an offset of 10 μm from the fiber axis, and the channel parameters were measured by moving the receiver alignment stage over the set of positions shown in the inset of Fig. 1. Using the channel matrix, the achievable data rate was calculated with the formula from (3), and plotted in Fig. 7 for 10 m, 100 m, 500 m, 1 km and 3 km fiber sections. A two-dimensional cross-section is also displayed for better comprehension of the plot. Although 10 μm may not be the optimal offset at the transmit stage to maximize the achieved data rate, the study of how the achievable data rate varied at the receiver serves to illustrate the spatial sensitivity of the detector offset, and how this sensitivity changes with the length of the fiber section.

The results in Fig. 7 allow us to draw some interesting inferences. It is easy to see that the maximum achievable data rate falls with increasing fiber length, owing to fiber losses and additional dispersion. Having no offset causes a drop in the data rate since there is insufficient modal spread among the transmitted data in order to support multiple streams. In addition, the alignment tolerances for achieving the maximum data rate are more stringent for shorter fiber lengths, and are more relaxed for longer fiber lengths. For instance, to achieve 95% or more of the maximum achievable 25 Gb/s for the 10 m case shown in Fig. 7(a), the tolerance turns out to be ± 2 μm, while for the 18.7 Gb/s in the 3 km case, this number rises to ± 6 μm. This can be attributed to spreading of the modal content into more neighboring modes (that have similar spatial characteristics) as the fiber section lengths increase progressively [45]. Such mode mixing did not significantly affect the performance of signal processing using linear techniques, since the group velocities of these neighboring modes are very similar.

Fig. 7 provides a picture of how the offset coupling affects data rate performance for a fixed launch configuration. Fig. 8 characterizes the relationship between the receiver stage offset for different offset launch configurations. The "effective SNR" plotted in the figure is the SNR that is obtained for the best stream after performing a MIMO equalization procedure (corresponding to the highest singular value). As is noted in [17], the optimal receiver offsets that maximizes the processed effective SNR is fairly close to the transmitter offset.

Overall, the results from Figs. 7 and 8 indicate that a significant improvement in data rate can be obtained with appropriate

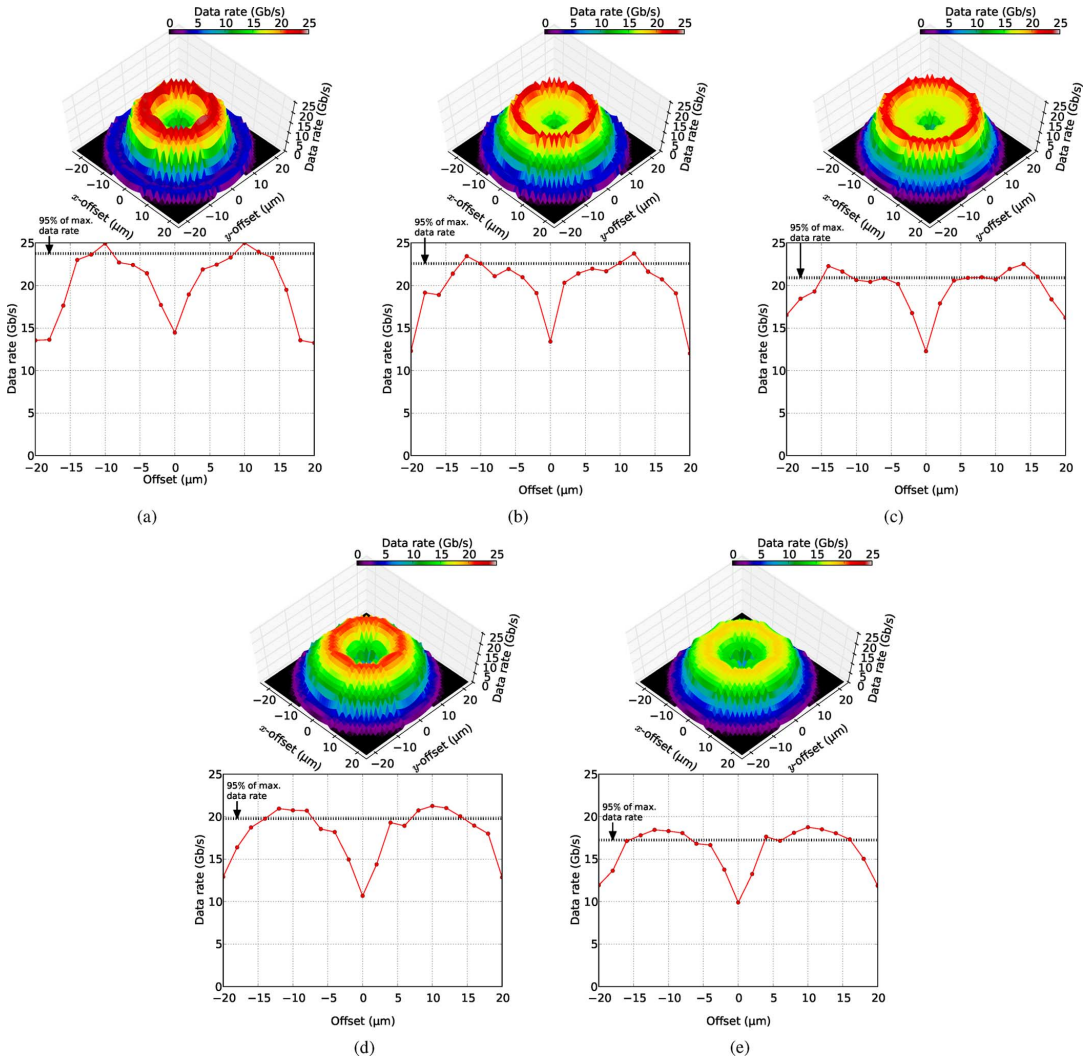

Fig. 7. The radial variation of the capacity for various detector alignment stage offsets for a fixed position of the transmitter side alignment stage, in 3-dimensions above as well as the cross-section along a plane below. As can be seen, an increase in length reduces the achievable data rate, but increases the tolerance with which the receiver stage needs to be aligned. (a) 10 m, (b) 100 m, (c) 500 m, (d) 1 km, (e) 3 km.

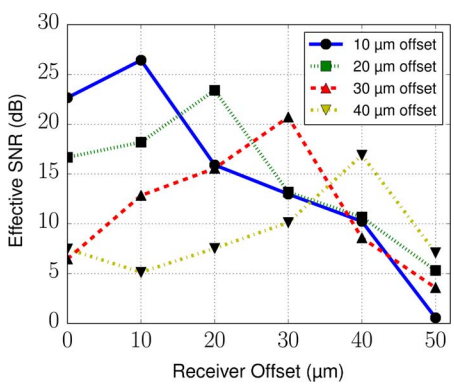

Fig. 8. The effective (MIMO processed) SNR for the best multiplexed stream obtained at the receiver for various transmit offset configurations. The best receiver offset for each case is fairly close to the launch offset.

signal processing and offset coupling with a fair amount of tolerance to misalignments. In the feedback based spatial multiplexing case, by setting the transmit and receive alignment stages to a 10 μm of offset, we were able to attain within 5% of the maximum data rate obtained with optimized offsets of the receiver alignment stage for each fiber section length. In addition, the power received did not vary much once the alignment stages were set to the optimal position, as has been observed in related experiments [17], [43]. Thus, even MMF systems with fixed offsets that would be simpler to deploy would be able to realize significant gains with the use of MIMO techniques like the ones described here, while retaining relaxed alignment tolerances.

2) Data Rates Without Channel State Feedback: For each fiber section, the positions of both of the optical alignment stages at the transmit and receive ends were moved across the 40 μm $\times$ 40 μm square grid with points separated by 2 μm, as shown in Fig. 1, and, for the offset settings in which the best channel quality was obtained, the data rate was evaluated. To evaluate all possible configurations of the offset stages, the transmit stage was initially set to one of the 441 grid locations indicated by the dots, and the receiver parameters were measured for each of the 441 points. This was then repeated for each of the transmit stage positions. Table II lists the optimal offset positions of the fiber alignment stages at the transmitter

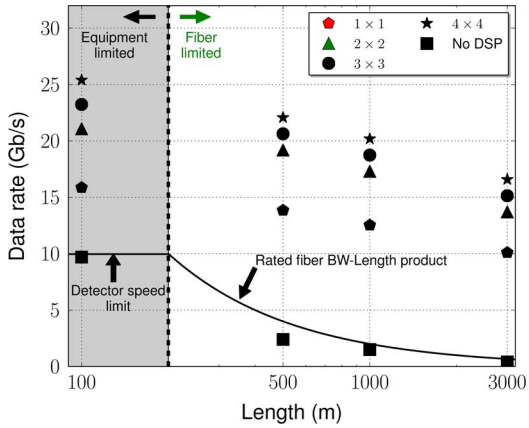

Fig. 9. Data rate versus length for various lengths of fiber with V-BLAST. These data rates were observed with optimized offset launch and detection with V-BLAST. The solid curve indicates the rated fiber bandwidth-length product, while the dotted line indicates the saturation speed for the detector beyond which the eye diagram shows a mostly closed eye.

TABLE II
OPTIMAL AXIAL OFFSETS FOR 4 × 4 SYSTEM

MMF Length	Transmit stage	Receive stage	Tolerance
10 m	14 μm	12 μm	±2 μm
100 m	12 μm	10 μm	±2 μm
500 m	10 μm	8 μm	±4 μm
1 km	10 μm	10 μm	±4 μm
3 km	12 μm	12 μm	±6 μm

and receiver where the highest data rate was obtained. The tolerance is defined as the minimum offset that can be tolerated at the transmitter or receiver that causes the data rate to fall below 95% of the maximum. The best axial offsets for each length were in between 8 μm to 12 μm at both the transmitter and receiver alignment stages, and the data rate did not vary appreciably with small perturbations, as discussed previously. The data rate was evaluated for the best offsets using V-BLAST decoding without channel state feedback to the transmitter, the data rates obtained are shown in Fig. 9.

The performance with on-off keying and no additional dispersion compensation, as used in standards such as 10 GBASE-LRM, is labeled "No DSP" in Fig. 9. The bandwidth of the generated signals was smaller than the full bandwidth supported by the fiber at lengths of 200 m or less, since the speed of the modulators, photodetectors and the waveform generators was limited to 7 GHz. The impact of this limitation is indicated by the shaded region in the left part of Fig. 9. For longer fiber lengths, fiber dispersive effects became more pronounced, and signal processing techniques enabled data rates to significantly exceed the rated bandwidth-length product of the fiber. The fiber channel responses were measured for each data stream using the pilot sequences, and the best offsets for the two fiber-alignment stages were those that maximized the total data rate. A sample-averaged SNR for the 4 × 4 system with a 3 km fiber section is shown in Fig. 10. For most situations, an axial offset of ∼10 μm from the fiber center at both the launch and detection stages was found to be effective for increasing the data rate for all fiber lengths considered. The temporal variation of the channel was sufficiently slow and the change in the best offset

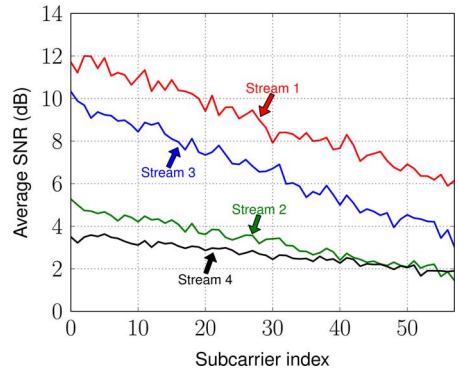

Fig. 10. Average SNR for each stream in the 3 km 4 × 4 case, corresponding to the data streams labeled x_1, x_2, x_3 and x_4 in Fig. 1. The energy of each subcarrier was averaged over 100 OFDM symbols for an SNR estimate.

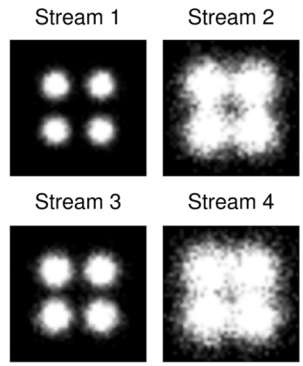

Fig. 11. Constellations received in the 35th subcarrier over a 3 km 4 × 4 link with offset launch and detection that correspond to the data streams labeled x_1, x_2, x_3 and x_4 in Fig. 1. While streams 1 and 3 have a very low BER ($\sim 10^{-5}$), 2 and 4 suffer from a much higher BER ($\sim 10^{-2}$).

location was not significant (as in [3], [43]), allowing for estimation and equalization digital compensation of dispersion and intermodal coupling while fixing fiber offsets. Once the best fiber alignment parameters were established, random bits were generated for each data stream and transmitted over the optical link. Upon reception, the signals were processed offline to evaluate the BER. A sample received constellation on subcarrier 35 for a 4 × 4 MIMO link over a 3 km MMF section is presented in Fig. 11. Here, it can be observed that V-BLAST decoding results in two streams (in this case, streams 1 and 3) that possess a much lower BER than the other two. Even though the average power received at each photodetector was roughly the same (around −5 dBm), streams 1 and 3 outperform streams 2 and 4. This is because x_1 and x_3 possess a higher effective SNR when decoding them from the signals received on all of the photodetectors combined. After decoding these, the remaining interference due to intermodal coupling was too great for V-BLAST decoding to recover x_2 and x_4. The performance observed in streams 1 and 3 was similar to that which can be obtained in wireless MIMO systems, where two channels seen by a pair of appropriately spaced antennas possess significant spatial diversity [27]. In the optical case, the spatial separation between these streams is provided using alignment stages. Conversely, for streams 2 and 4, the incremental benefits mirror the wireless MIMO case for antennas that are not appropriately spaced,

resulting in heavily correlated channels and diminished diversity gains [27]. This suggests that the benefits offered by controlled spatial offsets of fiber axes significantly exceed those from the inherent spatial diversity offered by couplers and mode scramblers.

Next, the data rates supported by the system for various MIMO configurations and various fiber lengths with V-BLAST was observed. To verify the efficacy of the system in compensating for differential model delay for higher order modes, the 1×1 system was evaluated with several offsets, and dispersion compensation was found to be effective up to offsets of 22 μm. Subsequently, the performance evaluation was conducted for all relevant MIMO configurations, as described in III.A. The modulation and coding rates were adjusted to obtain a coded BER of 10^{-9} and the measured BER was then verified to be within this limit by averaging bit-error counts over several transmissions. The data rate improvement from the 1×1 to 2×2 case was significant, but diminished benefits were obtained with further increase in the numbers of transmitters/receivers, due to the lack of additional modal diversity. From observing the performance versus fiber length, it is evident that effective signal processing with MIMO was able to increase data rates through the MMF link, ranging from 26 Gb/s to 16.5 Gb/s for 4×4 systems with lengths increasing from 100 m through 3 km. Significantly, MIMO signaling and signal processing was able to increase data rates to 16.5 Gb/s over 3 km, exceeding the bandwidth-length product by 25-fold in comparison to 10 GBASE-SR data rates. The same improvement was not observed at shorter fiber lengths due to the bandwidth limitations of the waveform generators and photodetectors. The use of faster components that raise the bandwidth limitation from the current 7 GHz to 10 GHz is expected to provide up to 30% increase in data rates for lengths of 200 m or less [1]. Equipment limitations notwithstanding, the trends observed at all lengths confirm the benefits of using MIMO-based multiplexing to effectively boost the data rate in MMF links. Offset launch was able to provide a consistent 60–70% increase in data rates at all lengths, thus underscoring the benefits of the higher modal diversity harnessed from offset launch and detection.

3) Data Rates With Channel State Feedback: A similar evaluation of data rates was performed for the case of spatial multiplexing with feedback. For each of the cases, it was observed that, upon parallelizing the channels to obtain virtual channels and ordering these based on singular values, the first two channels were usable, and the remaining two were very noisy, and did not support a high data rate. This is indicative of the fact that the predominant benefit of the fiber offsets is effectively captured in the first two virtual channels. The highest possible QAM constellation was used in these channels to maximize the data rate, and error control coding was used to keep the BER below 10^{-9}. The data rates obtained are shown in Fig. 12. Although only two virtual channels were used, the data rates supported on them were higher than those obtained in the case of V-BLAST by about 12%. Fig. 13 shows two constellations obtained after transmission over the best virtual channels for the 1 km case, where the ability to transmit a rich constellation (QAM-64) over the primary virtual channel compensates for the inaccessibility

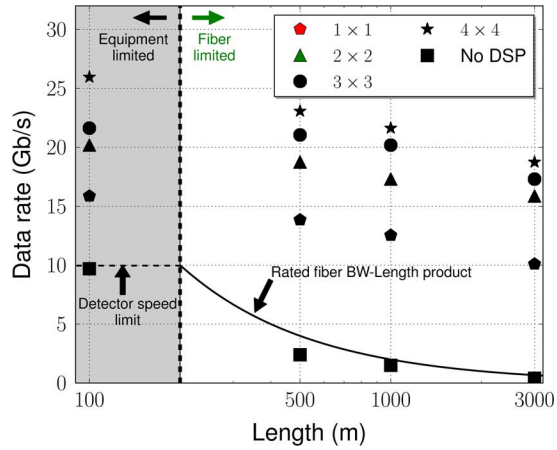

Fig. 12. Data rate versus length for various lengths of fiber with spatial multiplexing. These data rates were observed with optimized offset launch and detection with spatial multiplexing with feedback of channel coefficients.

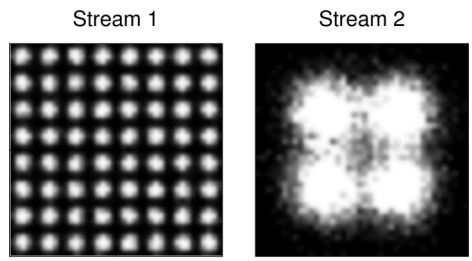

Fig. 13. Constellations for the two virtual channels which were used for modulation with feedback based spatial multiplexing for a 1 km MMF. (a) Stream 1 (highest singular value): a QAM-64 constellation was supported by this virtual channel. (b) Stream 2 (second highest singular value): Only a QAM-4 constellation was supported in this virtual channel. The remaining two channels were ignored, since their SNRs were very low.

of the remaining two channels. The ability to use a constellation with higher spectral efficiency is a notable improvement over the V-BLAST case, owing the the availability of feedback of channel state information to the transmitter. The singular values realized for the four virtual channels, with the largest singular value normalized to unity, were [1.00, 0.33, 0.04, 0.001], thus making the effective SNRs of the second, third and fourth channels respectively 10 dB, 28 dB and 60 dB lower than the first. The observation that only the first two channels are usable and that the two had a very low SNR can be understood by realizing that we had the flexibility of only one offset each at the transmitter and receiver, thus possessing only one spatial degree of freedom with full control in addition to direct center launch. The flexibility to introduce more axial offset streams to effectively utilize different modes of the fiber is likely to increase the third and fourth singular values as well, making them useful for multiplexing by endowing them with a higher effective SNR.

Optimal axial offsets of the alignment stages at the transmitter and receiver were ~ 8 μm and did not vary much with length, possibly due to the inherently large beam size of the VCSEL output. The alignment tolerance, measured as the maximum offset introduced at the transmitter or receiver for the data rate to reduce by 5%, was about 2 μm up to 100 m and 4 to 6 μm

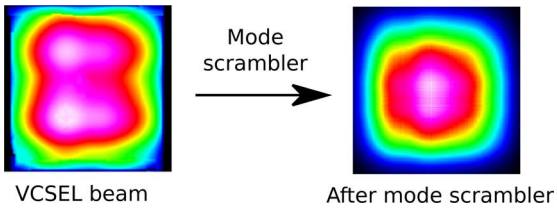

Fig. 14. Initial VCSEL beam pattern and after being shaped by a mode scrambler.

for lengths of 500 m and above. The results of the data rate experiments for the spatial multiplexing case are shown in Fig. 12. For 100 m and 500 m, the data rate increase is not significant in comparison to the V-BLAST data rates, as shown in Fig. 9. This is likely because the benefits obtained with spatial multiplexing with a simple (noisy) channel quantization might prove insufficient to harness the full benefits of parallelizing the channels with channel state feedback. However, for the 1 km and 3 km cases, the data rate improves noticeably, by 5% and 10% respectively. While these data rate improvements are modest, the value of these techniques is indicative of further benefits which can be exploited with more sophisticated feedback techniques in optical links. Using V-BLAST and spatial multiplexing with offset coupling, a bandwidth-length product of about 57 Gb/s-km (for the 3 km case) was obtained, representing an improvement of 28-fold over the rated fiber bandwidth-length parameter of the fiber.

B. 2 × 2 Link Over Silica MMF With VCSELs

An experiment similar to the one conducted with the DFB laser setup was conducted with directly modulated VCSELs for the 2×2 case, as shown in Fig. 3. However, the fiber lengths were restricted to 1 km, since the power emitted by each laser (-3 dBm) was insufficient to support a 3 km MIMO link with an acceptable SNR at 3 km.

The VCSELs had an cross-section diameter of 40 μm, which caused them to emit beams that were several times larger than the beams obtained in the DFB case. Moreover, the resulting beam is shaped according to the inherent spatial mode pattern of the emitting laser. As shown in Fig. 14, passing the signal through a mode scrambler was effective in shaping the beam, although the impact on data rate due to this transformation was not appreciable. Thus, the ability attract a diversity of modes among the two transmitted signals to improve multiplexing performance is greatly diminished.

A procedure similar to that of the DFB link was performed for the evaluation of channel parameters, and by varying the modulation and coding for the position with highest rate. The rate was evaluated by substituting channel parameters in (3). For the position that provided the highest rate, the modulation and coding parameters were optimized, and the best obtainable data rate was measured. The results are shown in Fig. 15, where the rated fiber bandwidth-length product is 1 Gb/s, and "Sp. mux." refers to the performance using spatial multiplexing with feedback. The signal processing and multiplexing benefits are able to exceed the bandwidth length product significantly for links of 100 m or more, but the benefits are significantly diminished in comparison to the DFB case. In addition, while feedback and spatial multiplexing improved data rate performance for the 500 m and 1 km cases, the benefits are small. For example, examining the 35th subcarrier reveals that the ratio of the second singular value to the highest one diminishes from 0.55 to 0.18 as the length ranges from 10 m to 1 km. As a result, 10 Gb/s could not be reached for the 1 km case, and the bandwidth-length product increase over the rated fiber parameter of 1 Gb/s was restricted to $9\times$; much less than the $28\times$ improvement obtained in the DFB 4×4 case. This diminished performance can be attributed to two major effects. First, the larger core diameter of the VCSEL beams causes the power loss with offset coupling to be more severe, thereby limiting gains due to MIMO. Second, the large beam size also limits control over the number of separate mode groups that are excited, thus causing a significant correlation among the two data streams. The use of VCSELs with smaller beam sizes and more effective strategies for offset launch with VCSELs would improve multiplexing performance.

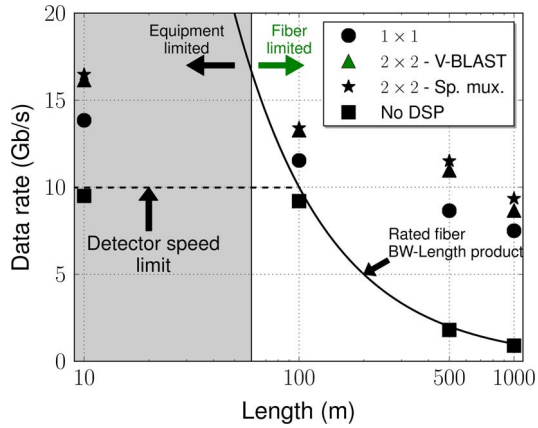

Fig. 15. Data rate performance of the 2×2 VCSEL link. The benefits from spatial multiplexing are not very significant, although there is notable improvement at longer fiber lengths.

C. 2 × 2 Link With Plastic MMF

The channel parameters and data rate performance was evaluated with plastic fibers in a manner similar to the measurements conducted with silica fibers, as described in the earlier subsections. However, due to the lossy, dispersive nature of the plastic fibers, the lengths of fiber sections for which the experiments were conducted were restricted to 1 m, 10 m and 100 m. In addition, for these experiments, the waveform generators were operated in their "interleaved" mode, wherein each waveform generator generated a 20 gigasamples/s signal.

The optimal fiber alignment stage offsets at the transmitter and receiver were ~ 8 μm and did not change much with the plastic fiber length. The alignment tolerance, measured as the maximum offset introduced at the transmitter or receiver for the data rate to reduce by 5%, was about 4 μm for all lengths. The data rates measured in this experiment are shown in Fig. 16, where the rated fiber bandwidth-length product is 200 Mb/s-km, and "Sp. mux." refers to the performance using spatial multiplexing with feedback. An interesting observation is that spatial multiplexing does not improve the performance significantly in comparison to V-BLAST. More significantly, the benefits

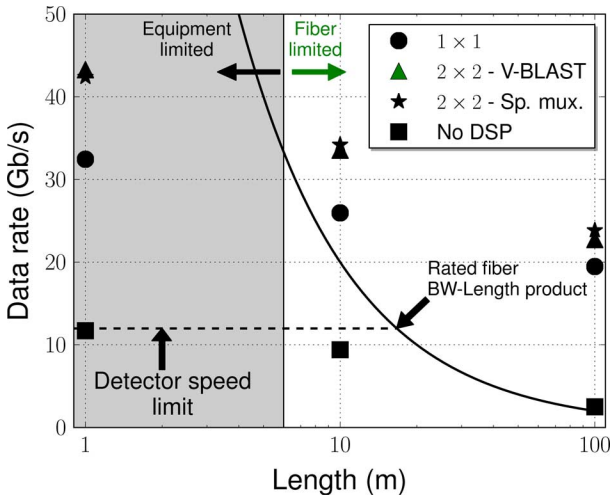

Fig. 16. Data rate performance of the 2 × 2 plastic fiber link.

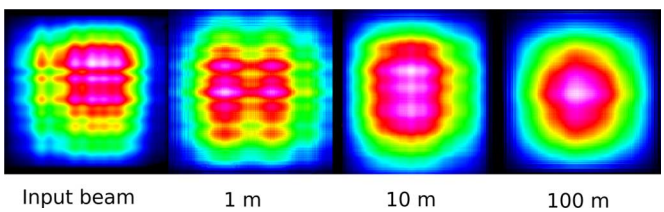

Fig. 17. Beam propagation in plastic fiber sections of various lengths. The heavy intermodal coupling causes a spatial spread of the signal even within tens of meters.

from multiplexing display a diminishing trend at longer lengths of fiber. For instance, the 35th subcarrier sees the ratio of the second singular value to the highest one diminish as 0.65, 0.53 and 0.2 for a 1 m section, 10 m and 100 m respectively. This is indicative of the fact that the multiplexing capabilities of the channel are poorer than in the silica case, likely due to significant intermodal coupling in 100 m of plastic fiber. This is consistent with earlier observations of significant mode coupling over short distances of perfluorinated plastic fiber [46], [47]. For a visual manifestation for this effect, Fig. 17 shows the impact on a beam launched from a glass fiber patch cord (referred to as "Input") into the plastic fiber sections used in this experiment. It is clear that even as the distance rises to about 10 m, the beam spreads significantly across the cross section of the fiber, thus indicative of the signal spreading across several modes. In terms of the singular values of the MIMO channel, the second singular value was significantly diminished at 10 m, and almost negligible at 100 m. Thus, the bandwidth-length product increase is restricted to about 12×.

In view of these observations, multiplexing through plastic fibers seems to offer significant benefits only at short distances. At lengths longer than tens of meters, while signal processing without MIMO (the 1 × 1 case in Fig. 16) remains effective, the benefits of multiplexing seem to diminish significantly. Thus, the bandwidth-length product improvement can be attributed largely to advanced modulation and signal processing, as opposed to multiplexing, for long sections of plastic MMF.

V. Discussion

In this section, we discuss the observations and results presented in the previous section, and comment on what the implications of these results are for some of the practical aspects of designing components and signal processing for realizing efficient and effective MIMO-MMF systems.

The first realization, based on the experimental results, is that the use of linear processing techniques such as V-BLAST and spatial multiplexing are effective in increasing data rates in intensity modulation/direct detection based links. The use of offset coupling and mode scramblers with these processing techniques boosts MIMO performance with incoherent detection. However, these improvements are not as significant as the data rate increases observed in coherent optical MIMO links, where a linear growth in data rates is generally observed with increasing number of modulator/detector pairs [5], [10], [11]. The use of direct detection reduces the effectiveness of multiplexing through modes of the fiber. Although coherent detection is more effective in increasing data rates, deployment of such a solution would impose significant cost and complexity, thus making it a less attractive proposition for short, inexpensive fiber optic links. Future work should involve a detailed comparison of cost, complexity and data rate with coherent and incoherent detection, and determine the system limits where the utility of each technique lies.

The use of feedback in optical links is relevant, especially since most optical links involve a bidirectional setup, thus providing very high bandwidth paths from both transmitters to receivers. Moreover, since channel conditions vary slowly in comparison to the data rates, the amount of feedback can be made very small (of the order of 0.1%). The feedback methods used in the experiments described in this paper to enable channel parallelization using spatial multiplexing are simplistic due to constraints in implementation, yet they offer evidence of the utility of providing channel state information to the transmitter. A further refinement of techniques to estimate and effectively quantize and transmit channel state information can be expected to provide further increases in performance and the flexibility to enable a larger number of streams of data through the MMF with high effective SNRs.

Evaluating the power consumption of the silica link described in the previous section with an estimate for the DSP power requirements, we find that over the range of 100 m to 3 km, the energy-per-bit achievable with the 4 × 4 MIMO link is between 0.15 to 0.25 nJ/bit. This number is comparable to the current energy-per-bit values achieved in data centers and access networks [48]. However, signal processing also affords us techniques such as dynamic rate and power adaptation [15] that widens the scope for achieving power savings in these links. Implementing these techniques and evaluating the power savings that can be obtained by efficient link utilization is a topic currently under investigation.

Finally, the effectiveness of offset launch and detection in conjunction with signal processing facilitates a significant increase the data rates in MMF links. Due to equipment limitations, only one alignment stage was employed at the transmitter, and one at the receiver. For a fixed offset at the transmitter, the

TABLE III
SUMMARY OF EXPERIMENTAL RESULTS

Fiber/Laser Setup	MIMO	BW-length product
Silica MMF, DFB	4×4	57 Gb/s-km ($28\times$ rated)
Silica MMF, VCSEL	2×2	9 Gb/s-km ($9\times$ rated)
Plastic MMF, FPL	2×2	2.4 Gb/s-km ($12\times$ rated)

results from the experiments described in Section IV provide only two effective streams even in a 4×4 configuration. This indicates that using only one offset launch stage each at the transmitter and receiver with mode scramblers is insufficient to exceed support more than two parallel multiplexed streams. These observations are also consistent with other experimental observations on the characteristics of systems that use offset launch in with MMFs. For instance, a similar conclusion on the effectiveness of exciting more than two mode groups is made in [22], although the focus there is on bandwidth-length product enhancement without multiplexing.

In spite of these limitations, the observations from these experiments strongly indicate that using offset coupling and signal processing makes multiplexing effective, and the ability to launch multiple data streams, with the flexibility of axial offsets and greater modal diversity, promises to further increase data rates. While the use of complicated alignment solutions, such as nanoprecision fiber alignment stages provides significant control and accuracy, it is not practical to use these tools when deploying such links. However, the results from Section IV indicate that there is a significant amount of flexibility and tolerance in positioning the launch and detection stages for optimal data rates, motivating the design of devices such as arrays of lasers and detectors with appropriate geometries to harness modal diversity benefits. The use of such devices would provide a convenient and and easily deployable solution that would enable multiplexing through MMF links.

VI. CONCLUSION

The use of conventional multimode fibers has been limited, owing to the data rate restrictions imposed by modal dispersion. While electronic dispersion compensation enables some improvement in data rates, a further boost requires techniques such as advanced modulation, signal processing and techniques such as MIMO. To gain a better understanding of how various parameters of the system, such as offset coupling, fiber channel parameters and different optical components affect system performance, we have performed an extensive experimental characterization of the fiber channel for various fiber media over several fiber sections of various lengths. In addition to a thorough evaluation of the fiber channel parameters, we have also presented an evaluation of various modulation and feedback methods that are able to provide bandwidth-length product increases ranging from $10\times$ to $28\times$, with the bandwidth-length products are summarized in Table III. The observed data rates ranged from 16–25 Gb/s with DFB lasers and VCSELs on silica fibers with lengths of 100 m to 3 km. While plastic fibers exhibited significant intermodal coupling at longer lengths, MIMO techniques still enabled a $12\times$ improvement in data rate, achieving 22 Gb/s over 100 m. While the use of mode scramblers enhanced data rates in a 4×4 system, only two streams could be transmitted effectively. Future work should investigate how multiple axially offset streams can be used to overcome diversity limits, and motivate the design of arrays of lasers and detectors that can take advantage of modal diversity. In addition, investigations are needed to study how improved feedback quantization can improve the performance of spatial multiplexing for better preprocessing of data symbols at the transmitter.

REFERENCES

[1] G. P. Agrawal, *Fiber-Optic Communication Systems*. New York, NY, USA: Wiley, 1997.

[2] H. R. Stuart, "Dispersive multiplexing in multimode optical fiber," *Science*, vol. 289, 2000.

[3] A. R. Shah, R. C. J. Hsu, A. Tarighat, A. H. Sayed, and B. Jalali, "Coherent optical MIMO (COMIMO)," *J. Lightw. Technol.*, vol. 23, no. 8, pp. 2410–2419, Aug. 2005.

[4] A. Tarighat, R. C. Hsu, A. Shah, A. H. Sayed, and B. Jalali, "Fundamentals and challenges of optical multiple-input multiple-output multimode fiber links [topics in optical communications]," *IEEE Commun. Mag.*, vol. 45, no. 5, pp. 57–63, 2007.

[5] R. Ryf, S. Randel, A. Gnauck, C. Bolle, R. Essiambre, P. Winzer, D. Peckham, A. McCurdy, and R. Lingle, "Space-division multiplexing over 10 km of three-mode fiber using coherent 6×6 MIMO processing," in *Proc. OFC*, 2011, pp. 1–3.

[6] J. Sakaguchi, Y. Awaji, N. Wada, A. Kanno, T. Kawanishi, T. Hayashi, T. Taru, T. Kobayashi, and M. Watanabe, "109-Tb/s ($7 \times 97 \times 172$-Gb/s SDM/WDM/PDM) QPSK transmission through 16.8-km homogeneous multi-core fiber," in *Proc. OFC*, 2011, pp. 1–3.

[7] B. Zhu, T. Taunay, M. Fishteyn, X. Liu, S. Chandrasekhar, M. Yan, J. Fini, E. Monberg, and F. Dimarcello, "Space-, wavelength-, polarization-division multiplexed transmission of 56-Tb/s over a 76.8-km seven-core fiber," in *Proc. OFC*, 2011, pp. 1–3.

[8] A. Li, A. Al Amin, X. Chen, and W. Shieh, "Reception of mode and polarization multiplexed 107-Gb/s CO-OFDM signal over a two-mode fiber," in *Proc. NFOEC*, 2011, pp. 1–3.

[9] M. Salsi *et al.*, "Transmission at 2×100 Gb/s, over two modes of 40 km-long prototype few-mode fiber, using LCOS based mode multiplexer and demultiplexer," in *Proc. NFOEC*, 2011, pp. 1–3.

[10] S. Randel *et al.*, "6×56-gb/s mode-division multiplexed transmission over 33-km few-mode fiber enabled by 6×6 mimo equalization," *Opt. Exp.*, vol. 19, no. 17, pp. 16 697–16 707, 2011.

[11] R. Ryf *et al.*, "Mode-division multiplexing over 96 km of few-mode fiber using coherent 6×6 MIMO processing," *J. Lightw. Technol.*, vol. 30, no. 4, pp. 521–531, 2012.

[12] S. Jansen, I. Morita, and H. Tanaka, "10×121. 9-Gb/s PDM-OFDM transmission with 2-b/s/Hz spectral efficiency over 1 000 km of SSMF," in *Proc. OFC*, 2008, Optical Society of America.

[13] S. Jansen, I. Morita, and H. Tanaka, "16×52. 5-Gb/s, 50-GHz spaced, POLMUX-CO-OFDM transmission over 4 160 km of SSMF enabled by MIMO processing," in *Proc. 2007 33rd European Conference and Exhibition of Optical Communication-Post-Deadline Papers (Published 2008)*, 2007, pp. 1–2.

[14] Y. Ma, Q. Yang, Y. Tang, S. Chen, and W. Shieh, "1-Tb/s single-channel coherent optical OFDM transmission with orthogonal-band multiplexing and subwavelength bandwidth access," *J. Lightw. Technol.*, vol. 28, no. 4, pp. 308–315, 2010.

[15] W. Shieh, Q. Yang, and Y. Ma, "107 Gb/s coherent optical OFDM transmission over 1000-km SSMF fiber using orthogonal band multiplexing," *Opt. Exp.*, vol. 16, no. 9, pp. 6378–6386, 2008.

[16] C. Tsekrekos, A. Martinez, F. Huijskens, and A. Koonen, "Mode group diversity multiplexing transceiver design for graded-index multimode fibres," in *Proc. 31st European Conference on Optical Communication, 2005. ECOC 2005.*, 2005, vol. 3, pp. 727–728, IET.

[17] H. Chen, H. van den Boom, and A. Koonen, "30-Gb/s 3×3 optical mode group-division-multiplexing system with optimized joint detection," *IEEE Photon. Technol. Lett.*, vol. 23, pp. 1283–1285, 2011.

[18] S. Schöllmann, N. Schrammar, and W. Rosenkranz, "Experimental realisation of 3×3 MIMO system with mode group diversity multiplexing limited by modal noise," in *Proc. OFC*, 2008, pp. 1–3.

[19] K. Appaiah, S. Vishwanath, and S. R. Bank, "Advanced modulation and multiple-input multiple-output multimode fiber links," *IEEE Photon. Technol. Lett.*, vol. 23, no. 20, pp. 1424–1426, 2011.

[20] B. Thomsen, "MIMO enabled 40 Gb/s transmission using mode division multiplexing in multimode fiber," in *Proc. OFC*, 2010, pp. 1–3, IEEE.

[21] S. Schöllmann and W. Rosenkranz, "Experimental equalization of crosstalk in a 2×2 MIMO system based on mode group diversity multiplexing in MMF systems@10.7 Gb/s," in *Proc. 2007 33rd ECOC*, 2007, pp. 1–2.

[22] L. Raddatz, I. White, D. Cunningham, and M. Nowell, "An experimental and theoretical study of the offset launch technique for the enhancement of the bandwidth of multimode fiber links," *J. Lightw. Technol.*, vol. 16, no. 3, p. 324, 1998.

[23] R. Giddings, X. Jin, and J. Tang, "First experimental demonstration of 6 Gb/s real-time optical OFDM transceivers incorporating channel estimation and variable power loading," *Opt. Exp.*, vol. 17, no. 22, pp. 19 727–19 738, 2009.

[24] S. Lee, F. Breyer, S. Randel, O. Ziemann, H. van den Boom, and A. Koonen, "Low-cost and robust 1-Gbit/s plastic optical fiber link based on light-emitting diode technology," in *Proc. OFC*, 2008, pp. 1–3.

[25] H. Yang, S. Lee, E. Tangdiongga, C. Okonkwo, H. van den Boom, F. Breyer, S. Randel, and A. Koonen, "47.4 gb/s transmission over 100 m graded-index plastic optical fiber based on rate-adaptive discrete multitone modulation," *J. Lightw. Technol.*, vol. 28, no. 4, pp. 352–359, 2010.

[26] N. Raptis, E. Grivas, E. Pikasis, and D. Syvridis, "Space-time block code based mimo encoding for large core step index plastic optical fiber transmission systems," *Opt. Exp.*, vol. 19, no. 11, pp. 10 336–10 350, 2011.

[27] D. Tse and P. Viswanath, *Fundamentals of Wireless Communication*. Cambridge, U.K.: Cambridge Univ Press, 2005.

[28] B. Schmidt, A. Lowery, and J. Armstrong, "Experimental demonstrations of electronic dispersion compensation for long-haul transmission using direct-detection optical OFDM," *J. Lightw. Technol.*, vol. 26, p. 196, 2008.

[29] W. Shieh and I. Djordjevic, *OFDM for Optical Communications*. New York, NY, USA: Academic, 2009.

[30] W. Shieh and I. Djordjevic, *OFDM for Optical Communications*. New York, NY, USA: Academic, 2009.

[31] Q. Yang, A. Al Amin, and W. Shieh, "Optical OFDM basics," in *Impact of Nonlinearities on Fiber Optic Communications*. New York, NY, USA: Springer, 2011, pp. 43–85.

[32] J. Tang and K. A. Shore, "Maximizing the transmission performance of adaptively modulated optical OFDM signals in multimode-fiber links by optimizing analog-to-digital converters," *J. Lightw. Technol.*, vol. 25, no. 3, pp. 787–798, 2007.

[33] E. Giacoumidis, S. K. Ibrahim, J. Zhao, J. Tang, A. D. Ellis, and I. Tomkos, "Experimental and theoretical investigations of intensity-modulation and direct-detection optical fast-ofdm over MMF-links," *IEEE Photon. Technol. Lett.*, vol. 24, no. 1, pp. 52–54, 2012.

[34] A. Goldsmith, *Wireless Communications*. Cambridge, U.K.: Cambridge Univ. Press, 2005.

[35] J. Siuzdak, "RF carrier frequency selection for incoherent MIMO transmission over MM fibers," *J. Lightw. Technol.*, vol. 27, no. 22, pp. 4960–4963, 2009.

[36] M. Kowalczyk and J. Siuzdak, "Four-channel incoherent MIMO transmission over 4.4-km MM fiber," *Microw. Opt. Technol. Lett.*, vol. 53, no. 3, pp. 502–506, 2011.

[37] Z. Haas and M. Santoro, "A mode-filtering scheme for improvement of the bandwidth-distance product in multimode fiber systems," *J. Lightw. Technol.*, vol. 11, no. 7, pp. 1125–1131, 1993.

[38] C. Cole, D. Allouche, F. Flens, B. Huebner, and T. Nguyen, "100 gbe-optical lan technologies [applications & practice]," *IEEE Commun. Mag.*, vol. 45, no. 12, pp. 12–19, 2007.

[39] M. Tokuda, S. Seikai, K. Yoshida, and N. Uchida, "Measurement of baseband frequency response of multimode fibre by using a new type of mode scrambler," *Electron. Lett.*, vol. 13, no. 5, pp. 146–147, 1977.

[40] W. Shieh, X. Yi, Y. Ma, and Q. Yang, "Coherent optical OFDM: Has its time come?," *J. Opt. Netw.*, vol. 7, 2008.

[41] J. Armstrong, "OFDM for optical communications," *J. Lightw. Technol.*, vol. 27, no. 3, pp. 189–204, 2009.

[42] P. W. Wolniansky, G. J. Foschini, G. Golden, and R. A. Valenzuela, "V-blast: An architecture for realizing very high data rates over the rich-scattering wireless channel," in *Proc. URSI Int. Symp. Signals, Systems, Electronics*, 1998, pp. 295–300.

[43] C. Tsekrekos, M. de Boer, A. Martinez, F. Willems, and A. Koonen, "Temporal stability of a transparent mode group diversity multiplexing link," *IEEE Photon. Technol. Lett.*, vol. 18, no. 23, pp. 2484–2486, 2006.

[44] D. Love, R. Heath, V. Lau, D. Gesbert, B. Rao, and M. Andrews, "An overview of limited feedback in wireless communication systems," *IEEE J. Sel. Areas Commun.*, vol. 26, no. 8, pp. 1341–1365, 2008.

[45] M. Shemirani, W. Mao, R. Panicker, and J. Kahn, "Principal modes in graded-index multimode fiber in presence of spatial and polarization-mode coupling," *J. Lightw. Technol.*, vol. 27, no. 10, pp. 1248–1261, 2009.

[46] S. Golowich, W. White, W. Reed, and E. Knudsen, "Quantitative estimates of mode coupling and differential modal attenuation in perfluorinated graded-index plastic optical fiber," *J. Lightw. Technol.*, vol. 21, no. 1, pp. 111–121, 2003.

[47] X. Quan, L. Blyler, and W. White, "Plastic optical fibers: Pipe-dream or reality?," in *Proc. ACS Symposium Series*, 2001, vol. 795, pp. 25–34.

[48] R. Tucker, R. Parthiban, J. Baliga, K. Hinton, R. Ayre, and W. Sorin, "Evolution of WDM optical IP networks: A cost and energy perspective," *J. Lightw. Technol.*, vol. 27, no. 3, pp. 243–252, 2009.